Journal of General Virology (2016), **97**, 1350–1355 DOI 10.1099/jgv.0.000452

Short Communication

Neurotropism of Saffold virus in a mouse model

Frédéric Sorgeloos,[1]† Cécile Lardinois,[2]† Sophie Jacobs,[2] Frank J. M. van Kuppeveld,[3] Bernd Kaspers[4] and Thomas Michiels[2]

Correspondence
Thomas Michiels
thomas.michiels@uclouvain.be

[1]Department of Pathology, Addenbrooke's Hospital, University of Cambridge, Hills Road, Cambridge, UK

[2]de Duve Institute, Université Catholique de Louvain, VIRO B1.74.07, 74 Avenue Hippocrate, Brussels B-1200, Belgium

[3]Moleculaire Virologie, Universiteit Utrecht, Yalelaan 1 Kamer W.512, 3584 CL Utrecht, The Netherlands

[4]Institut für Tierphysiologie, Veterinärstr 13, 80539 München, Germany

Received 8 December 2015
Accepted 7 March 2016

Saffold virus (SAFV) is a highly seroprevalent human *Cardiovirus* discovered recently. No clear association between SAFV infection and human disease has been established. Rare infection cases, however, correlated with neurological symptoms. To gain insight into the pathogenesis potential of the virus, we performed experimental mouse infection with SAFV strains of genotypes 2 and 3 (SAFV-2 and SAFV-3). After intraperitoneal infection, both strains exhibited a typical *Cardiovirus* tropism. Viral load was most prominent in the pancreas. Heart, spleen, brain and spinal cord were also infected. In IFN-receptor 1 deficient (IFNAR-KO) mice, SAFV-3 caused a severe encephalitis. The virus was detected by immunohistochemistry in many parts of the brain and spinal cord, both in neurons and astrocytes, but astrocyte infection was more extensive. *In vitro*, SAFV-3 also infected astrocytes better than neurons in mixed primary cultures. Astrocytes were, however, very efficiently protected by IFN-α/β treatment.

Saffold virus (SAFV) was isolated from a stool sample of a child who presented with fever of unknown origin in 1981. In 2007, the virus was sequenced and identified as a *Cardiovirus* of the species *Theilovirus*, presenting the highest nucleotide identity with rat Theilovirus (RTV), a *Theilovirus* isolated from rats (Jones *et al.*, 2007). SAFV is the first *Theilovirus* that was clearly identified as a human virus. Other *Theilovirus* members are neurotropic viruses: Theiler's murine encephalomyelitis virus (TMEV), isolated from mouse; RTV; and Vilyuisk human encephalomyelitis virus, whose possible human origin is unclear (Lipton, 2008). A subset of TMEV strains (persistent strains) have the intriguing ability to establish a persistent infection in the white matter of the central nervous system (CNS) despite a robust immune response of the host (Brahic *et al.*, 2005). When the virus persists in the CNS, it is responsible for an inflammatory demyelinating pathology that is reminiscent of human multiple sclerosis (MS) (Oleszak *et al.*, 2004). A recent study attempted to detect SAFV genomes in active brain lesions of MS patients, but results were negative (Galama *et al.*, 2014). Also, no reactivity to SAFV was detected in oligoclonal bands of MS patients' cerebrospinal fluid (CSF). *In vitro*, SAFV was reported to be able to persistentlyinfect HeLa cell cultures (Himeda *et al.*, 2013). A serological survey revealed that SAFV-3 and SAFV-2 (Chiu *et al.*, 2010; Galama *et al.*, 2011) seroprevalence can reach more than 90 % in the adult population, and that the infection occurs early in life (mainly before the age of two) (Zoll *et al.*, 2009). SAFV strains are circulating worldwide as seroprevalence was very high in America (Chiu *et al.*, 2010), Europe, Africa and Asia (Zoll *et al.*, 2009). Up to now, 11 different genotypes have been identified, with SAFV-1, SAFV-2 and SAFV-3 being the most prevalent (Drexler *et al.*, 2008; Khamrin *et al.*, 2013; Nielsen *et al.*, 2012b; Tapia *et al.*, 2015). The virus was detected in the stools and respiratory samples of both symptomatic (gastrointestinal and respiratory symptoms) and asymptomatic patients. It was also detected in the stools of some patients presenting with acute flaccid paralysis (Naeem *et al.*, 2014), and in the CSF and myocardium of a child who died suddenly with no history of illness (Nielsen *et al.*, 2012a). However, no causative association between SAFV infection and any human pathology has been firmly established.

In order to get new insights into the pathogenesis potential of SAFV, we performed experimental mouse infection with virus strains belonging to the genotypes 2 and 3 that were isolated previously (Zoll *et al.*, 2009). Handling of mice (agreement LA1230472) and experimental procedures were

†These authors contributed equally to this work.

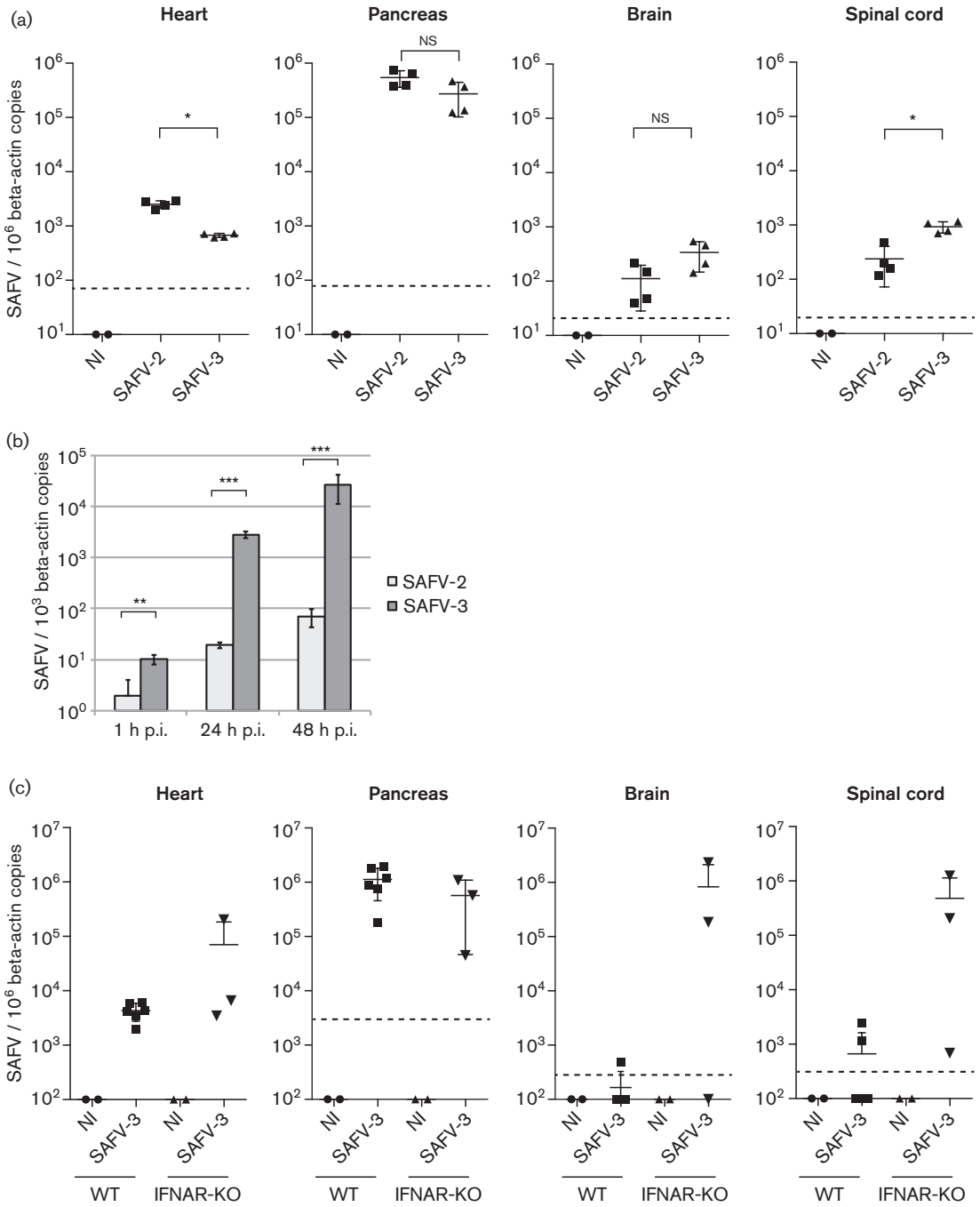

Fig. 1. SAFV tropism. (a) Quantification, by RT-qPCR, of the viral load (mean and SD) in heart, pancreas, brain and spinal cord of 129/Sv mice, 7 days after IP inoculation. Plots show the number of SAFV genome cDNA copies per 1×10^6 β-actin cDNA copies detected in one experiment for individual mice infected with SAFV-2 (squares; n=4), with SAFV-3 (triangles; n=4), or left non-infected (NI) (circles; n=2). Dashed lines indicate the technical limit of detection. (b) Propagation of SAFV-2 and SAFV-3 on primary murine neuron cultures. Hippocampal neurons (100 000) isolated from WT CD1 mice were grown on coverslips and infected at an m.o.i. of 0.01. Viral replication was followed by RT-qPCR. Graphs show the mean and SD of the number of virus cDNA copies per 1000 β-actin cDNA copies detected by RT-qPCR at 1, 24 and 48 h post-infection (p.i.). A similar infection experiment performed at 8, 12 and 16 h p.i. yielded similar data. The number of genomes in SAFV-2 and SAFV-3 inoculums, measured by RT-qPCR, was equivalent (not shown). (c) RT-qPCR quantification of SAFV-3 (mean and SD) in heart, pancreas, brain and spinal cord, 7 days after IP inoculation of WT 129/Sv mice (n=6) or 10 days after IP inoculation of IFNAR-KO mice (n=3). Scatterplots show the data for individual mice in one infection experiment. Results are expressed as SAFV genome cDNA copies per 1×10^6 β-actin cDNA copies. Dashed lines indicate the technical limit of detection. Note that

among SAFV-3 infected IFNAR-KO mice, viral load correlated among different organs (i.e. the mouse that had the highest viral load in the brain also had the highest viral load in other organs). Statistics: Mann–Whitney two-tailed test (*$P<0.05$; **$P<0.01$; ***$P<0.001$; NS, non- significant).

conducted in accordance with the EEC (European Economic Community) directive 86/609/CEE and the related Belgian law of 6 April 2010. The study and protocol used in this study were approved by the ethics committee of the University of Louvain under the agreement no. 2010/UCL/MD/031. Three-week-old 129/Sv female mice were inoculated by the intraperitoneal (IP) route with 10^5 $TCID_{50}$ of SAFV-2 (n=4) or SAFV-3 (n=4) or were mock-infected (n=2). IP inoculation was chosen because it provides the virus access to peripheral tissues, while allowing testing of the neuroinvasive properties of the virus. Mice failed to develop clinical symptoms. Seven days post-infection (p.i.), viral load was quantified in different organs by reverse-transcription and quantitative PCR (RT-qPCR), using the SYBR Green method (Fig. 1a). Primers used to detect SAFV were 5′-TGTAGCGACCTCACAGTAGCA-3′ (sense) and 5′-CAGGACATTCTTGGCTTCTCTA-3′ (antisense). Primers used to detect mRNA encoding β-actin were described previously (Sommereyns *et al.*, 2008).

SAFV-2 and SAFV-3 exhibited a similar tropism. Viral genome was detected in the heart, pancreas, spleen, brain and spinal cord, but not in the intestine and thymus (Fig. 1a and data not shown). This pattern fits with the typical tropism of other Cardioviruses. Infection of the pancreas was striking and warrants further studies on the potential infection of this organ by SAFV in humans. The virus also showed some neuroinvasive potential, since both SAFV-2 and SAFV-3 viruses were detected in the brain and spinal cord after IP inoculation. Of note, SAFV-3 appeared to be slightly more neurotropic than SAFV-2 as viral load was slightly higher for SAFV-3 than for SAFV-2 in CNS and slightly lower in the other tissues. *In vitro*, in primary hippocampal neuron cultures prepared by the protocol of Fath *et al.* (2009), SAFV-3 also replicated more efficiently than SAFV-2 (Fig. 1b).

Some TMEV strains have a striking ability to persist in the CNS of susceptible mice (Brahic *et al.*, 2005). Susceptibility notably depends on the haplotype of the mice as H-2^b mice were shown to clear TMEV infection by mounting a strong cytotoxic T lymphocyte response against an immunodominant epitope present in the VP2 capsid protein and conserved among TMEV and SAFV strains (Dethlefs *et al.*, 1997). To assess the ability of SAFV to persist in the CNS, FVB/N mice (H-2^q haplotype) were inoculated intracerebrally with 10^5 $TCID_{50}$ SAFV-2 (n=5) or SAFV-3 (n=5), and viral load was measured by RT-qPCR in brain and spinal cord, 6 weeks after inoculation. This mouse strain was previously shown to be susceptible to SAFV-2-mediated early encephalitis after intracranial inoculation (Hertzler *et al.*, 2011). At 45 days p.i., SAFV-2 was almost undetectable ($1.8 \pm 0.3\times10^1$ SAFV per 10^6 β-actin cDNA copies) and SAFV-3 was present at a very low titre ($2.4 \pm 1.9\times10^2$ SAFV per 10^6 β-actin cDNA copies) in the brain. Neither SAFV-2 nor SAFV-3 was detected in the spinal cord ($< 10^1$ SAFV per 10^6 β actin cDNA copies). Also, upregulation of the IFN-stimulated *Oasl2* gene, measured by RT-qPCR (Sommereyns *et al.*, 2008), was weak (< three fold) in SAFV-inoculated mice, suggesting that very little viral replication was ongoing 45 days post-inoculation. Thus, SAFV-2 and SAFV-3 have a much lower ability to persist in the mouse CNS than persistent TMEV strains.

We next characterized the tropism of SAFV-3 in the CNS. Therefore, infection of WT 129/Sv mice (n=6) was repeated with a new SAFV-3 virus stock. In addition, a few (n=3) IFN-receptor 1-deficient 129/Sv mice (IFNAR-KO) were inoculated to evaluate the impact of type I IFN on neuroinvasion by SAFV (Fig. 1c).

As in the experiment described in Fig. 1(a), infection in WT mice was asymptomatic. Viral load was most prominent in the pancreas. Heart and spleen were also infected, but CNS infection only occurred in two out of six mice. Nevertheless, these data confirmed the neuroinvasive ability of SAFV-3 in the mouse model. In the case of IFNAR-KO mice, one mouse exhibited severe signs of encephalitis (ruffled fur, hunched back, ataxia) and had an extremely high viral load in the CNS and in other organs analysed. One asymptomatic IFNAR-KO mouse had a lower, yet elevated, viral load in the CNS, and one had a low viral load in all organs. Thus, for two out of three IFNAR-KO mice, CNS infection was particularly high, suggesting that the type I IFN response critically acts to control neuroinvasion. Influence of type I IFN was less striking in other tissues (Fig. 1c).

To define the cellular tropism of SAFV-3 in the CNS of IFNAR-KO mice, two antibodies were produced that allow SAFV detection by immunohistochemistry. A polyclonal chicken antibody was raised against the VP1 capsid protein of SAFV-3. For this purpose, SAFV-3 VP1 was purified from *Escherichia coli* as a His-tag fusion and used to immunize chickens. Polyclonal antisera were collected and tested for specificity on infected cell cultures. IgY was then purified from egg yolk as described elsewhere (Jensenius *et al.*, 1981). This antibody was used for immunohistochemistry (paraffin sections) at a dilution of 1/500. We also used a rabbit polyclonal antiserum directed against peptide CADYYKQRLIHDVEMNPG, which corresponds to the C-terminal 17 aa of TMEV (DA) 2A protein preceded by a cysteine residue that allowed conjugation to maleimide activated keyhole limpet haemocyanin (Pierce) before rabbit immunization (CER). The antiserum directed against TMEV 2A partly cross-reacted with SAFV 2A and allowed the detection of SAFV-infected cells in paraffin sections (Fig. 2g).

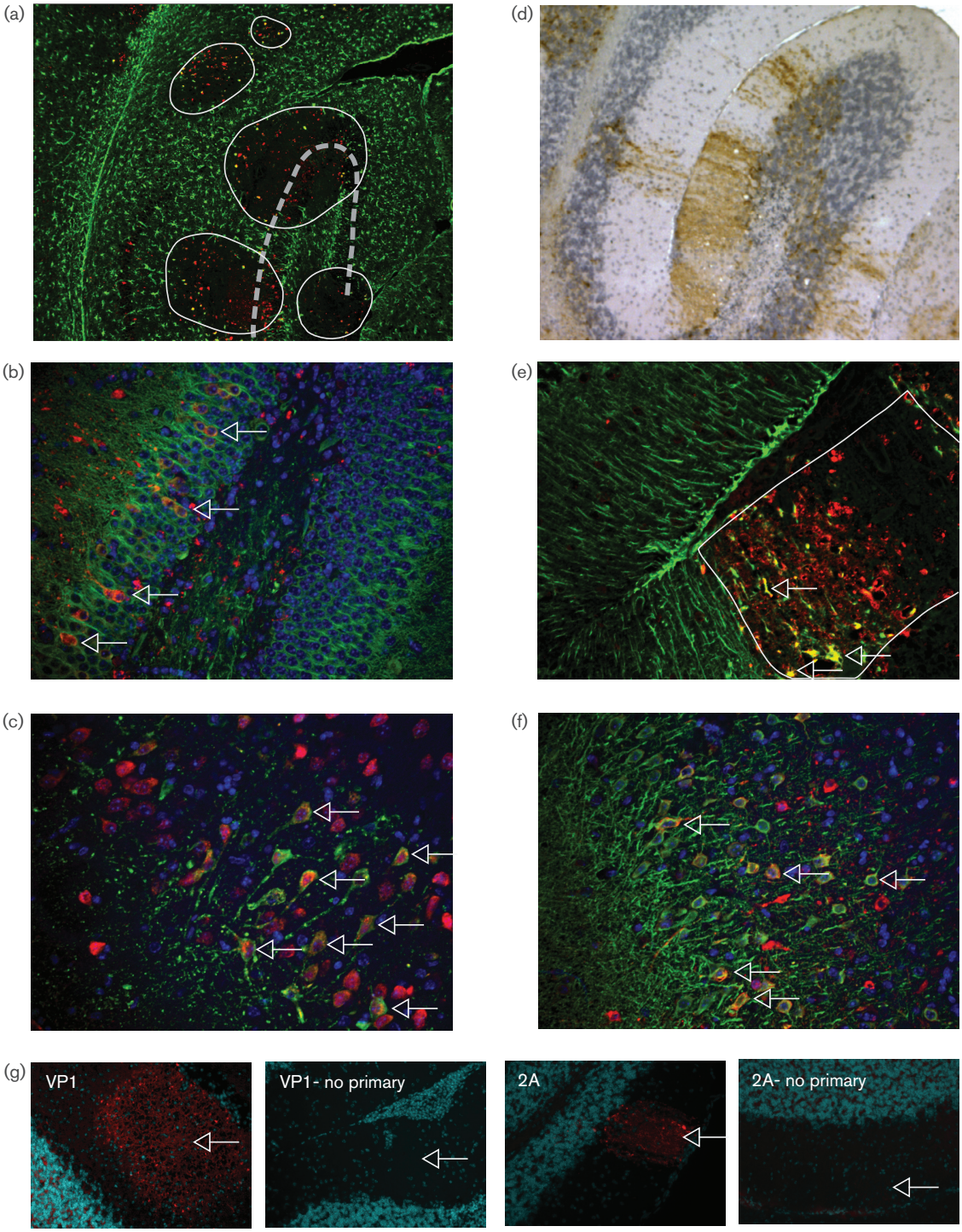

Fig. 2. SAFV-3 immunodetection in the brain of IFNAR-KO mice. (a) Low magnification image (width = 1.7 mm) showing extensive tissue damage in plaque-like infected areas (outlined by grey circles). Green, GFAP; red, SAFV-VP1. The dashed line shows the hippocampus location. (b) Confocal image showing infected neurons in the hippocampus. Green, MAP2; red, SAFV-VP1; blue, nuclei. Arrows point to typical doubly labelled cells. (c) Confocal image showing infected neurons in the cortex. Green, SAFV-VP1; red, NeuN; blue, nuclei. Arrows point to typical doubly labelled cells. (d) Low magnification image showing extensive infection (brown = SAFV 2A immunostaining with diaminobenzidine) of the Bergmann glia in the cerebellum. Nuclei were stained with hematoxylin. (e) Confocal image showing an infected area in the cerebellum, with extensive cell destruction (framed area). Green, GFAP; red, SAFV-VP1. Arrows point to typical doubly labelled cells. (f) Confocal image showing infected neurons in the cortex. Green, MAP2; red, SAFV-VP1. Arrows point to typical doubly labelled cells. (g) Control

labellings. Sections from a SAFV-3-infected cerebellum. Arrows point to areas where tissue damage is visible under green autofluorescence (not shown). Nuclei are pseudocoloured in light blue. SAFV labelling (red) from left to right: (i) SAFV-VP1, (ii) SAFV-VP1 with primary antibody omitted, (iii) 2A, (iv) 2A with primary antibody omitted.

For immunostaining, WT and IFNAR-KO 129/Sv mice were IP infected with 10^5 $TCID_{50}$ SAFV-3. After sacrifice, brains and spinal cords were collected and embedded in paraffin. Sections were immunolabelled with anti-VP1 or anti-2A antibodies, and with antibodies directed against cell-specific markers: astrocytes (GFAP; Dako), neuron (MAP2; Synaptic Systems; or NeuN; Millipore). WT mice developed no symptoms and viral antigen was not detected in analysed sections (not shown). In contrast, 6 days after IP infection, all IFNAR-KO mice (n=4) developed severe encephalitis symptoms (ruffled fur, hunched posture, paralysis) comparable to those of the heavily infected mouse analysed above (Fig. 1c). Mice were thus sacrificed and tissues were processed for immunostaining. The virus was found in many parts of the brain and of the spinal cord. Viral antigen was detected in both neurons and astrocytes. Infected neurons were mostly detected in the cortex and the hippocampus (Fig. 2b, c, f). Astrocyte infection was, however, more pronounced, notably in the cerebellum, brainstem and thalamus where large infection foci that resemble plaques were observed (Fig. 2a). In the cerebellum, SAFV-3 caused extensive infection of the Bergmann glia (Fig. 2d, e).

In vitro, SAFV-3 also exhibited a marked tropism for astrocytes in mixed mouse primary neuron–astrocyte cultures. At 8, 16 and 24 h p.i. with 4 $TCID_{50}$ SAFV-3 per cell, viral antigen accumulated much more in GFAP-positive (astrocytes) than in MAP2-positive (neurons) cells (Fig. 3a–c). We reported previously that IFN-α/β treatment poorly protected primary mouse neurons against infection by the GDVII strain

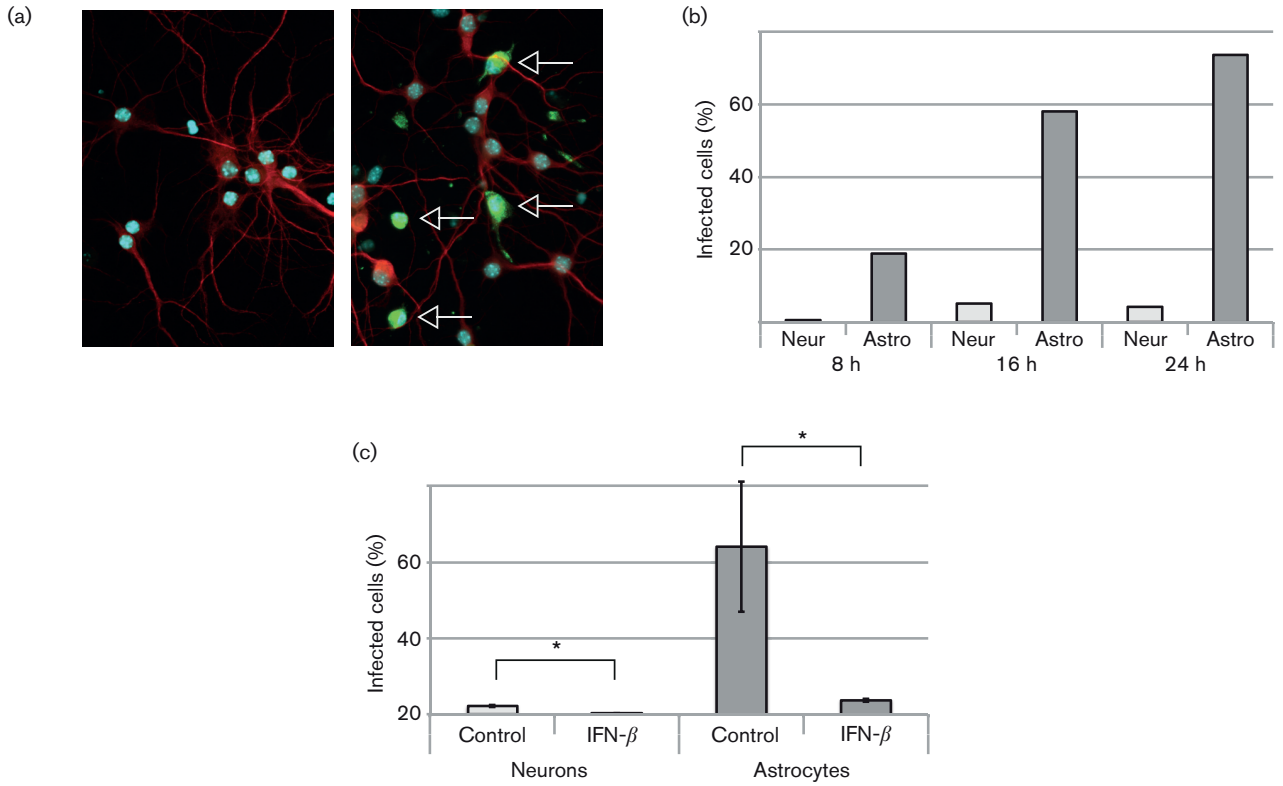

Fig. 3. IFN-β treatment protects astrocytes from SAFV infection. (a) Immunolabelling of SAFV-3-infected (right) and uninfected (left) neuron cultures showing the specificity of the anti-SAFV VP1 antibody (green labelling). Cells were fixed 16 h p.i. MAP2 is shown in red and nuclei in blue. Infected cells (green) are indicated by arrows. (b) SAFV-3 infection of mixed neuron–astrocytes cultures derived from WT CD1 mice. Graphs show the percentage of infected cells counted for each cell type, in a total of 20 microscope fields, taken from one infection experiment. (c) Mixed neuron–astrocytes cultures from WT CD1 mice were mock-treated or treated for 24 h with 10 IU IFN-β ml^{-1}, before infection for 12 h with SAFV-3. Graphs show the mean and SD of the percentage of infected neurons and astrocytes in an experiment involving three parallel culture infections. The biological influence of IFN-β treatment was confirmed in an independent experiment involving four parallel infections. *, P 0.05 by one-tailed Mann–Whitney test.

of TMEV (Kreit *et al.*, 2014). To test the protective effect of IFN against SAFV-3 in neurons and astrocytes, mixed cultures were treated for 24 h with 10 IU murine IFN-β ml^{-1} produced as described by Kreit *et al.* (2014) or with control medium, and then infected by SAFV-3 at an m.o.i. of 4. Twelve hours after infection, cells were fixed and immunolabelled as in the former experiment, and the percentage of infected cells was counted (Fig. 3c). Although visible, neuron protection was difficult to quantify, as the percentage of infected neurons was low. Astrocytes were strongly protected by IFN-β as the percentage of infected cells decreased by 12-fold after IFN-β treatment. Taken together, the *in vivo* and the *in vitro* data suggest that SAFV-3 has a pronounced tropism for astrocytes, but that these cells are strongly protected by the IFN response.

In conclusion, this work reports a preliminary characterization of SAFV tropism in the mouse model. Both SAFV-2 and SAFV-3 strains exhibit a pronounced tropism for the pancreas, which warrants further studies about the possible involvement of SAFV in pancreatic diseases in humans. In addition SAFV can infect the heart and the CNS, as expected for a member of the genus *Cardiovirus*. These observations are congruent with those of Kotani *et al.* (2016), which were published while this paper was in revision. These authors report the neuropathogenicity in mice, of two SAFV-3 clinical isolates. Our data further show that SAFV-3 exhibits a pronounced cellular tropism for astrocytes. These cells, however, appear to be potently protected from SAFV infection by the type I IFN response.

Acknowledgements

We are grateful to Muriel Minet for technical support in immunostainings and to Marguerite Kreit for help in neuron culture. C.L. was the recipient of a FRIA fellowship from the Belgian Fund for Scientific research. F.S. was supported by the DIANE convention of the Belgian Walloon region. S.J. was supported by Interuniversitary Attraction Poles programme initiated by the Belgian Science Policy Office (IAP-P7/45 BELVIR). Work was also supported by the ARC of the Communauté Française de Belgique and by the Belgian fund for Scientific Research (conv. 3.4519.11 and PDR T.0185.14).

References

Brahic, M., Bureau, J. F. & Michiels, T. (2005). The genetics of the persistent infection and demyelinating disease caused by Theiler's virus. *Annu Rev Microbiol* **59**, 279–298.

Chiu, C. Y., Greninger, A. L., Chen, E. C., Haggerty, T. D., Parsonnet, J., Delwart, E., Derisi, J. L. & Ganem, D. (2010). Cultivation and serological characterization of a human Theiler's-like cardiovirus associated with diarrheal disease. *J Virol* **84**, 4407–4414.

Dethlefs, S., Escriou, N., Brahic, M., van der Werf, S. & Larsson-Sciard, E. L. (1997). Theiler's virus and Mengo virus induce cross-reactive cytotoxic T lymphocytes restricted to the same immunodominant VP2 epitope in C57Bl/6 mice. *J Virol* **71**, 5361–5365.

Drexler, J. F., Luna, L. K., Stöcker, A., Almeida, P. S., Ribeiro, T. C., Petersen, N., Herzog, P., Pedroso, C., Huppertz, H. I. & other authors (2008). Circulation of 3 lineages of a novel Saffold cardiovirus in humans. *Emerg Infect Dis* **14**, 1398–1405.

Fath, T., Ke, Y. D., Gunning, P., Götz, J. & Ittner, L. M. (2009). Primary support cultures of hippocampal and substantia nigra neurons. *Nat Protoc* **4**, 78–85.

Galama, J. M., Zoll, J. G., Lanke, K. H., de Jong, A. S., Melief, J., Huitinga, I., Verbeek, M. M. & van Kuppeveld, F. J. (2014). Saffold cardiovirus and multiple sclerosis: no evidence for an association. *Ann Clin Transl Neurol* **1**, 618–621.

Galama, J., Lanke, K., Zoll, J., Roivainen, M. & van Kuppeveld, F. (2011). Seroepidemiology of Saffold cardiovirus type 2. *Emerg Infect Dis* **17**, 1572–1573.

Hertzler, S., Liang, Z., Treso, B. & Lipton, H. L. (2011). Adaptation of Saffold virus 2 for high-titer growth in mammalian cells. *J Virol* **85**, 7411–7418.

Himeda, T., Hosomi, T., Okuwa, T., Muraki, Y. & Ohara, Y. (2013). Saffold virus type 3 (SAFV-3) persists in HeLa cells. *PLoS One* **8**, e53194.

Jensenius, J. C., Andersen, I., Hau, J., Crone, M. & Koch, C. (1981). Eggs: conveniently packaged antibodies. Methods for purification of yolk IgG. *J Immunol Methods* **46**, 63–68.

Jones, M. S., Lukashov, V. V., Ganac, R. D. & Schnurr, D. P. (2007). Discovery of a novel human picornavirus in a stool sample from a pediatric patient presenting with fever of unknown origin. *J Clin Microbiol* **45**, 2144–2150.

Khamrin, P., Thongprachum, A., Kikuta, H., Yamamoto, A., Nishimura, S., Sugita, K., Baba, T., Kobayashi, M., Okitsu, S. & other authors (2013). Three clusters of Saffold viruses circulating in children with diarrhea in Japan. *Infect Genet Evol* **13**, 339–343.

Kotani, O., Naeem, A., Suzuki, T., Iwata-Yoshikawa, N., Sato, Y., Nakajima, N., Hosomi, T., Tsukagoshi, H., Kozawa, K. & other authors (2016). Neuropathogenicity of two Saffold virus type 3 isolates in mouse models. *PLoS One* **11**, e0148184.

Kreit, M., Paul, S., Knoops, L., De Cock, A., Sorgeloos, F. & Michiels, T. (2014). Inefficient type I interferon-mediated antiviral protection of primary mouse neurons is associated with the lack of apolipoprotein l9 expression. *J Virol* **88**, 3874–3884.

Lipton, H. L. (2008). Human Vilyuisk encephalitis. *Rev Med Virol* **18**, 347–352.

Naeem, A., Hosomi, T., Nishimura, Y., Alam, M. M., Oka, T., Zaidi, S. S. & Shimizu, H. (2014). Genetic diversity of circulating Saffold viruses in Pakistan and Afghanistan. *J Gen Virol* **95**, 1945–1957.

Nielsen, A. C., Bottiger, B., Banner, J., Hoffmann, T. & Nielsen, L. P. (2012a). Serious invasive Saffold virus infections in children, 2009. *Emerg Infect Dis* **18**, 7–12.

Nielsen, A. C., Gyhrs, M. L., Holmes, E. C. & Cui, J. (2012b). Co-circulation and persistence of genetically distinct saffold viruses, Denmark. *Emerg Infect Dis* **18**, 1694–1696.

Oleszak, E. L., Chang, J. R., Friedman, H., Katsetos, C. D. & Platsoucas, C. D. (2004). Theiler's virus infection: a model for multiple sclerosis. *Clin Microbiol Rev* **17**, 174–207.

Sommereyns, C., Paul, S., Staeheli, P. & Michiels, T. (2008). IFN-lambda (IFN-λ) is expressed in a tissue-dependent fashion and primarily acts on epithelial cells in vivo. *PLoS Pathog* **4**, e1000017.

Tapia, G., Bøås, H., de Muinck, E. J., Cinek, O., Stene, L. C., Torjesen, P. A., Rasmussen, T. & Rønningen, K. S. (2015). Saffold virus, a human cardiovirus, and risk of persistent islet autoantibodies in the longitudinal birth cohort study MIDIA. *PLoS One* **10**, e0136849.

Zoll, J., Erkens Hulshof, S., Lanke, K., Verduyn Lunel, F., Melchers, W. J., Schoondermark-van de Ven, E., Roivainen, M., Galama, J. M. & Van Kuppeveld, F. J. (2009). Saffold virus, a human Theiler's-like cardiovirus, is ubiquitous and causes infection early in life. *PLoS Pathog* **5**, e1000416.